

Surface-enhanced raman scattering nanostructures potential for biomedical applications

Abstract

Owing to the definitely excellent property of nanostructures such as controllable release of ions from the buried nanoscale thin layers, cell response to microscale morphological changes of substrates, distinctively enhancing sensitivity rendered by electrodes with sizes less than 10 micrometers, and dramatically increasing electromagnetic field from local surface plasmon resonance of nanostructures, nanostructures are playing more and more crucial role in the challenging fields. As one of the most sensitive spectroscopic tools, surface enhanced Raman scattering (SERS) shows highly sensitive biological and chemical detection, such as applications for a better biomedical applications and ecotoxicology. It is well known that surfaces with functioned nanostructures often possess the formation of surface plasma resonance resulted in SERS distinctive enhancement attractively. Therefore, nanostructures (such as nanorods and nanobranches/wires, nanofractal, nanoprisms, and hybrid nanostructures) for SERS are marked aim to provide the related vital information. It should be pointed out that there are a lot of substantial improvements related to the technical innovation in SERS fabrication with anisotropic nanostructures. However, obstacles or challenges are still to prevent these techniques from extensively applying in the practical applications, especially for the SERS-based systems. The significantly crucial case is that it is hard to control anisotropic nanoobjects assembly into ordered structures because the degree of order among the individual building blocks, spatial arrangement and the assembly direction determine the new and/or improved properties.

Keywords: nanostructure, surface-enhanced raman scattering, environmental application, nanorods, nanowires, nanoprisms, fractal, hybrid, anisotropic, ordered

Volume 4 Issue 4 - 2020

Kelvii Wei Guo

Department of Mechanical and Biomedical Engineering, City University of Hong Kong, china

Correspondence: Kelvii Wei Guo, Department of Mechanical and Biomedical Engineering, City University of Hong Kong, 83 Tat Chee Avenue, Kowloon Tong, Kowloon, Hong Kong, Email keliiguo@yahoo.com

Received: July 05, 2020 | **Published:** August 19, 2020

Introduction

Surface enhanced Raman scattering (SERS), as one of the most sensitive spectroscopic tools, shows highly sensitive biological and chemical detection. The tremendous efforts have been put into highly SERS-active substrates designed and fabricated with nano structured films and metallic nanoparticles because particle plasmon allows direct coupling of light to resonant electron plasmon oscillation. Theoretical investigation indicates that symmetry breaking resulting in along the structure and in gaps formed between these materials more intense electromagnetic field generated, permits for more complex plasmon propagation. As excellent candidates for SERS substrates, anisotropic metallic nanostructures possess all of the necessary characteristics. Hence, anisotropic materials are ideal for SERS. Since SERS discovered in 1973, it attracts more and more substantial attention.¹ Mean while, it makes a promising solution to solve the problem of the low sensitivity existed in the conventional Raman spectroscopy. SERS makes Raman spectroscopy more applicable to enhance the surface sensitivity. Moreover, it arouses the devotion of the investigation of the interfacial processes related to optical scattering enhanced from adsorbates on metal surfaces. In various kinds of fields from diagnostics to plasmonics, a worldwide effort has been put into optimizing, exploring and harnessing SERS spurring with the advent of SERS.²⁻⁵

The molecule and multi-amplification of the reradiated Raman scattered light excited in the local optical field are taken from an increment originated by predominantly electromagnetic SERS effect.⁶⁻¹¹ Usually, in most SERS systems, this optical enhancement is related to the surface plasmon oscillations excitation. Surfaces

with nanostructures commonly make the formation of the surface plasma resonance. When a laser beam is irradiated the metal surface with nanostructures, the light electromagnetic radiation coupled the metal surface and the free electrons confined on the metal surface in nanometer size coherently oscillated are taken as the localized surface plasma resonance. Such oscillation in the near-IR and visible-near UV region is spurring the intense absorption, UV-Vis spectroscopy can easily observe and record it. Research shows that the normal oscillation modes of the surface plasma resonance are resonant with both the excitation and the scattered photon for surface features smaller than the incident optical wavelength. The dielectric constant of the metal, determined the frequency of the surface plasma resonance, is the key to the SERS effects detected from only a few metals such as alkali metals, Au, Ag, and Cu.¹²⁻¹⁶ With the mechanism of SERS extensive exploring, SERS have an effective nanoscale effects in the field of nanoscience. When the nanostructures are agglomerated or distributed uniformly, the relevant intensity of SERS will be significantly decreased, for example, nanoparticles, nanorods, nanobranches and nano wires as the size of the constructed structures is much smaller than 10 nm or much larger than 100 nm. It is well known that the enhancement of SERS are mainly relied on the NPs morphology or their geometrical configuration, which means the aggregation can make the relevant plasmon resonance.¹⁷⁻¹⁹

Due to the light direct coupling with resonant electron plasmon oscillation for the particle plasmon, the substrates with metallic NPs and nanostructured films for highly SERS-activating are deeply designed and fabricated. At certain local junctions, the substrates sprayed with gold or silver colloids possess strong SERS signals. Results show that at nanoparticle junctions NPs coupled with intensively enhanced

electromagnetic field. To date, although at some local “hot spots” gold or silver colloid spraying on as substrate can achieve so-called high SERS signal to some extent, SERS spanning a wide dynamic range with uniform, stable, and reliable signal by this approach cannot be obtained easily. The relevant reason is the close-packed crystal-like structures and isolated particles are also the colloids components which show weak SERS enhancement. However, at present, the most investigation method is taken colloidal noble NPs as the bulk solution-based biochemical detection. For substrates, they should suffer from the reproducibility and the limited stability which are not suitable for the large-scale production of SERS-based sensors.^{20–22} Research illustrates complex plasmon propagation can be occurred more with the symmetry breaking, and in the gaps formed in these materials and along the structure more intense electromagnetic field generation is also occurred. Therefore, the anisotropic materials are ideal candidates for SERS. As the ideal candidates for SERS, anisotropic metallic nanostructures can realize (a) Bands of plasmon absorption can be controlled by controlling the aspect ratio of nanocrystals; (b) Symmetry breaking favoring for more complex plasmon propagation; (c) nanobranches, nanowires and nanorods aggregation or assembly can be fabricated easily resulted in the large field enhancement; (d) Functional architectures with anisotropic nanoobjects have attractive shape and size dependent properties; (e) The size of the sharp surface features and highly curved anisotropic nanostructures is less than 100 nm can improve the localized electromagnetic field up to a hundredfold.^{23–25}

Nanorods and nanobranches/wires

The current common anisotropic metallic nanostructures are shown innanobranches/wires and nanorods containing a long axis for inducing multipolar plasmon activity. Such structures have been designed and fabricated by many synthesis approaches.^{26–32} But, for 1D nanostructures are most hardly ordered. Although it can be achieved the amplified Raman spectra, the related mechanism of SERS is hard to be revealed. For fabricating the ideal SERS-active substrates with uniform nanobranches/wires arrays and nanorods, electron beam lithography with nano technique, a mature technique originating

from traditional contact printing technique has been applied to fabricate SERS-active substrate.³³ With the aid of the computer control of the size of the unit and the distance of intergaps precisely, effective SERS-active substrates from Au NPs and Aunanohole arrays were effectively achieved. Figure 1 shows different Aunanohole arrays with various diameters of units and the distances of intergaps and Table 1 lists the relevant nanohole arrays dimensions for comparison, where D : unit diameters, S : intergap distances, N_{surface} is the number of 4-MBA molecules adsorbed on the SERS-active area where the laser spot is irradiated, and EF: $EF = I_{\text{surface}} N_{\text{solution}} / I_{\text{solution}} N_{\text{surface}}$. I_{surface} and I_{solution} are 1077 cm^{-1} band intensities from the NP and nanohole array substrate and solution sample, respectively. N_{solution} is defined as the number of 4-mercaptobenzoic acid (4-MBA) molecules irradiated with the spot of laser, calculated as 5.34×10^8 with $78.5 \mu\text{m}^2$ of the size area of a laser spot and a packing density of 6.8×10^{14} 4-MBA molecules/ cm^2 . Meanwhile, 4-MBA was taken as probe molecules, and self-assembled on Aunanohole arrays to generate SERS spectra for the calculation of the enhancement to sure the influence of the size of the unit and the distance of the intergap on the SERS signals from various arrays.

It indicates that EF clearly increased with the decrement of the intergap distance with the constant nanohole diameter. However, the increment in the nanoholes diameter distinctively increased EF at the constant intergap distance, showing an opposite trend to that of in the Au nanoparticle arrays. The maximum EF, 8.61×10^6 , was obtained in Aunanohole arrays at a 125 nm intergap distance and 562 nm nanohole diameter, which can be compatible with the highest EF (1.08×10^7) received from the nanoparticle array with an intergap distance of 130 nm and a unit diameter of 90 nm. The results listed in Table 1 express a wide extent of intergap distances and nanohole arrays of nanohole diameters which obtained a high EF. The highest EF, 8.61×10^6 , was got in the Aunanohole array at an intergap distance of 125 nm, a unit diameter of 562 nm, and a hole depth of 300 nm. Moreover, it is considered a simpler task by this simple fabrication procedure to make unit diameters varying from 100 nm to 500 nm and an approximately 125 nm intergap distance for the nanohole arrays than to prepare the nanoparticle arrays.

Table 1 Au nanohole arrays: the calculated EF of SERS

Sample	D (nm)	S (nm)	SERS-active area (cm^2)	N_{surface}	Calculated EF
a	125	125	0.00289	4.29×10^8	7.60×10^4
b	125	312	0.00337	5.00×10^8	2.34×10^4
c	125	500	0.00349	5.17×10^8	1.94×10^4
d	312	125	0.00216	3.20×10^8	2.37×10^6
e	312	312	0.00289	4.29×10^8	2.31×10^6
f	312	500	0.00318	4.72×10^8	5.51×10^5
g	562	125	0.00171	2.53×10^8	8.61×10^6
h	562	312	0.00243	3.61×10^8	7.88×10^6
i	562	500	0.00281	4.17×10^8	5.86×10^6

Up to now, the investigation in this area for SERS is relatively rare. The main reason is probably that the regular nanostructures fabricating time is longer by these lithographic techniques. In addition, for the structures with high aspect ratio along with large area substrates, it is hard to obtain. Anodic aluminum oxide (AAO) templates, as another

important nanofabrication template synthesis technique, is reliable in organic solvents and at high temperature. The large arrays of nanobranches/wires and nanorods can be achieved by this method.^{34,35} The ease handling materials is primarily attractive. The A substrate gives both electrical contact and the mechanical support. The oxide

layer thickness can be easily tuned in the range of very thick to very thin. Controlling the reaction time can obtain different pore size of AAO templates and the applied voltage can control the pores density.

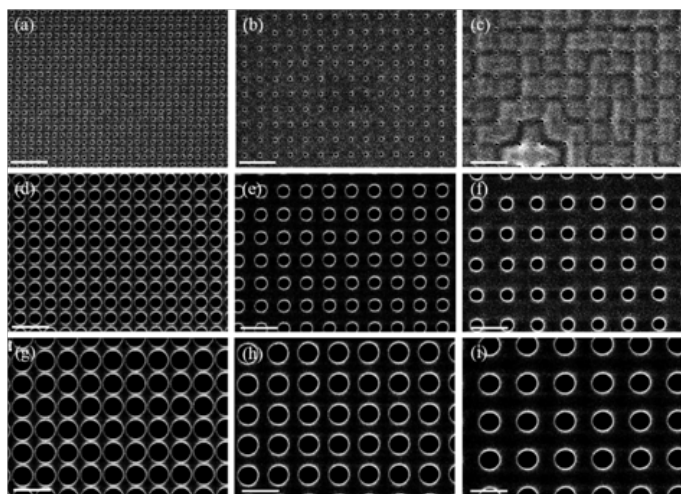


Figure 1 Aunanohole arrays with various dimensions.

Since 1995, AAO template has been used to make silver substrates for SERS. AAO template synthesis shows a door to the fabrication of ordered 1D nanostructured SERS substrates. Hao and coworkers developed a novel surface SERS-active substrate by electrode position in AgNO_3/PVP aqueous system with Ag-dendrites assembled on the surface and embedded in the channels of AAO membrane.³⁶ Figure 2 shows the mechanisms of the growth of Ag dendritic nanostructures. It reveals that Ag^+ ions in the electrolyte migrate to Ag foil surface, from the working electrode attain electrons and reduce to Ag^0 under the driving force of the electric field. Then clusters form when Ag atoms conglomerate. Meanwhile, the color of the silver foil becomes gray under the galvanic replacement reaction. After that, the reduction of Ag^+ is more serious as free electrons migrate to the surface of AAO via electron channel. Consequently, silver atoms nucleate on AAO surface and self-assemble as spherical aggregates. With PVP (as the agent of the functional capping) attached on the surfaces of crystal nucleus to adjust the growth of the oriented attachment and Ostwald ripening dominated Ag dendrites at the surface of AAO self-assembling, micro-silver dendrites are successfully obtained with high coverage.

Figure 3 expresses that the influence of the concentrations of AgNO_3/PVP solution on the silver dendrites growth. It can be seen that all the films of the dense Ag dendrite distribute on all over of the AAO supports surface. Furthermore, a distinctive structures with hierarchical dendritic characteristics stretch at least three branches at 0.06 M AgNO_3/PVP . Figure 3b and the inset illustrate that the sharp sub branches gradually disappear when the concentration of AgNO_3/PVP solution increases. While the concentration of AgNO_3/PVP solution increases further, the density of dendritic films becomes higher as shown in Figure 3c. It should be pointed out that three different kinds of dendritic structures with sharp branches even sub branches and uniform stems obtain at 0.1 M AgNO_3/PVP solution. Moreover, tremendous leaf-like flakes coating on the surface of earlier formed dendritic structures without distinct sub branches are also detected (inset in Figure 3c). More attractively, there are some branches self-assembling into hexagon plates as shown in lower right of inset of Figure 3c. The relationship between SERS signal

intensity and morphologies is shown in Figure 3d. It indicates that the intensity of SERS reduces with the increment of the reaction agents concentration. Because of the distinct multi generation spieric structure as well-defined, sharp branches and hierarchical surface roughness, the better enhancement of SERS of substrate obtains at 0.06 M AgNO_3/PVP solution.

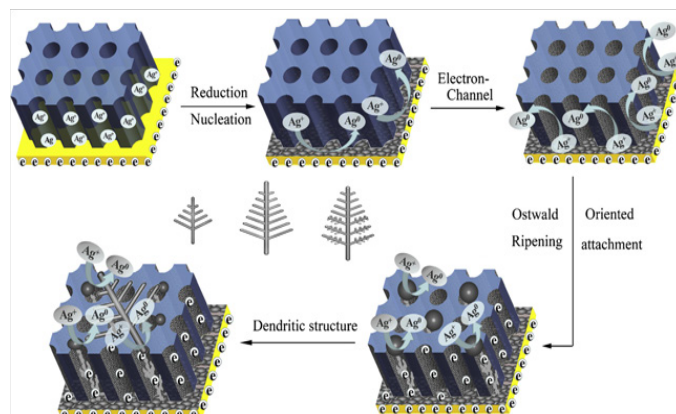


Figure 2 The proposed growth of silver dendritic.

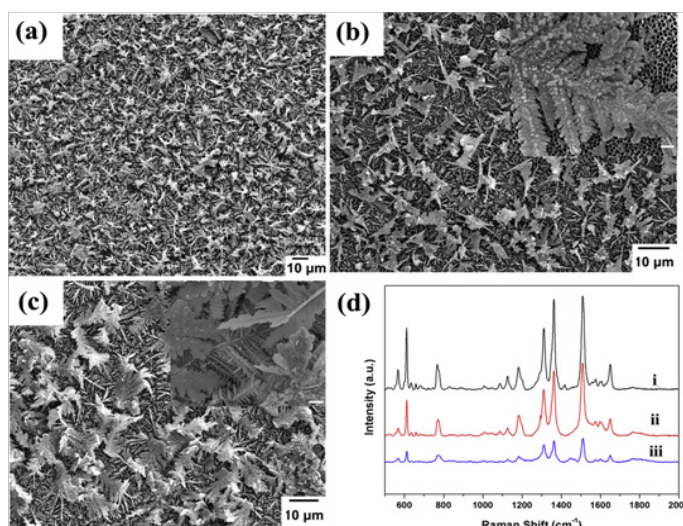


Figure 3 (a-c) Synthesized Ag dendrites at various AgNO_3/PVP solutions concentrations, (a) 0.06 M; (b) 0.08 M; (c) 0.1 M. (d) SERS spectra of 10^{-6} M R6G adsorbed on the various silver dendritic substrates: (i) 0.06 M; (ii) 0.08 M; (iii) 0.1 M.

TEM image of Ag dendrite and HRTEM image of the surface region of Ag dendrite are shown in Figure 4. It depicts that the inter-planar separation of Ag lattice fringes of the dendrite structures with identical crystal orientation is 0.235 nm as shown in Figure 4b, and its growth direction is dominated along $\{111\}$ plane. Also, the SAED pattern (the inset in Figure 4a) confirms the formation of single crystal convincingly. Research indicates that the size of a mean inter particle gap is as small as 5 ± 2 nm can be fabricated in silver rod-like nanoparticle arrays. The gaps precisely controlling in the sub 10 nm regime is crucial for achieving the attractive substrates with uniform high enhancement factors and better exploring or revealing the collective surface plasmons. However, for the present lithographic techniques, it is extremely hard. The same strategy has been shown to fabricate silver nano branches decorated with sputtered gold NPs

for SERS-active substrate.³⁷ Figure 5 shows silver nanobeads (NBs) attached with various thicknesses of gold nanoparticles (NPs). It can be seen that the AAO templates surface color varies obviously with the pulsed electrodeposition position of silver and the Al foils complete removal as shown in Figures 5a&5b shows Ag NBs distribute uniformly with high density on Ag nano wire arrays. Ag NBs embellish with different nominal thickness of Au NPs are shown in Figures 5c-5e. It shows that with the increment of the sputtered Au layers nominal thickness, gold NPs grow and the gaps between the neighboring Au NPs decrease spontaneously, the plasmonic coupling between adjacent gold NP enhancing.

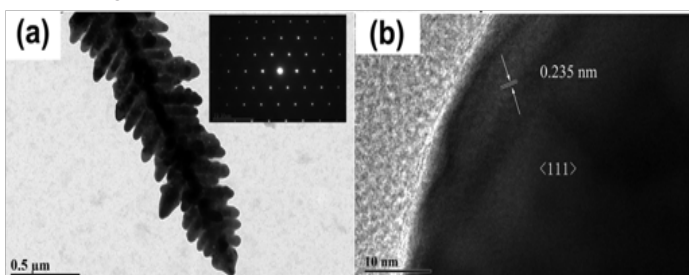


Figure 4 (a) Silver dendrite TEM image (b) Silver dendrite surface region HRTEM image.

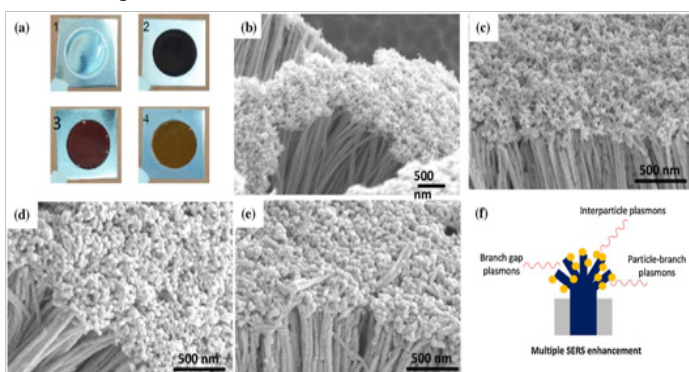


Figure 5 (a) Samples after 2nd anodization (1) pulsed electrodeposition (2) Al substrate removal (3) and AAO template partial dissolution (4); Gold nanoparticle-decorated silver nanobeads with nominal gold-thickness of (b) 0 nm, (c) 5 nm, (d) 15 nm, (e) 20 nm, (f) schematic diagram of multiple enhancements generated from gap plasmon couplings, particle-branch, and interparticle.

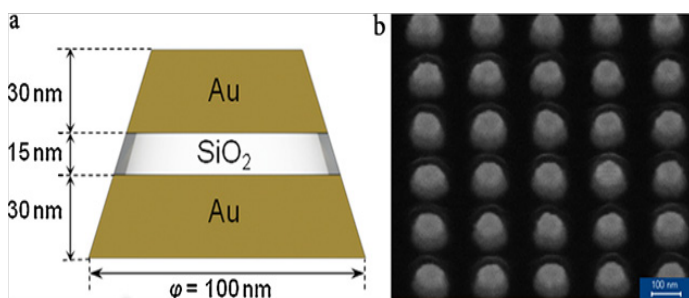


Figure 6 (a) A single nano-cone physical dimensions (b) An array of nano-cones with period of 200 nm and a base diameter of 100 nm.

Compared with silver NBs with only gap plasmons, Ag NBs embellished with NPs give synergistic plasmonic enhancements from branch gaps, particle-branch, and interparticle, resulted in a tremendous SERS effect as illustrated in Figure 5f. More interestingly, the intensity of SERS of Ag NBs embellished with Au NPs at 1079

cm^{-1} is ~ 10 times higher than that of silver nanobeads, indicating the definitely crucial effect of gold nanoparticles embellished on the silver nanobead substrate for the SERS effect enhancement.

For high SERS-active substrates, results indicate that the metal nanobranches/wires of the ordered transition with suitable dimensions are ideal candidates. In addition, silicon is also a crucial semiconducting material and its formed nanostructures are encouraging alternatives for future applications in integrated optoelectronic nanodevices. Up to now, by well-established silicon fabrication technology, the uniform silicon nanostructures with advanced characteristics can be easily synthesized. Consequently, silicon fabrication technology is considerably compatible with SERS substrate fabrication techniques, because by designing the desirable silicon nanostructures the performance of SERS can be effectively improved. The three main steps for Ag-coated Sinanorod and nano wire arrays are only needed. Firstly, by simple chemical etching, a silicon wafer dipped into an aqueous HF solution containing Ag^+ ions, high quality Sinanorods and nanowire arrays are fabricated. It includes Si wafer dissolution, Ag seed-induced excessive local oxidation, and subsequent 3-aminopropyltrimethoxysilane (APTMS) modification. With air drying, the APTMS-modified silicon nanorods and nanowire arrays are dipped into an aqueous solution containing Au NPs. On the surface of Si nanorods and nanowires, the small Au NPs are immobilized by the amine group. At last, to deposit silver, the resulting Au-decorated Si nanorods and nanowires arrays are immersed in a plating solution. By such approach, the silver deposition controlling can homogeneously achieve Ag film growth on Si nanowire arrays, which are beneficial to ultrasensitive molecular sensing with high SERS signal good stability, reproducibility, and enhancement ability.³⁸⁻⁴⁰

Nanofractal

Substrates with attractive fractal are quite complex. For the way to the more powerful and plentiful material resources, The “disordered” systems would be a better choice. With Mandelbrot first proposed fractal,⁴¹ research on both theoretical and application aspects is extensive explored. It is important to fabricate or optimize materials with different types of spectroscopy and nonlinear responses broadband amplification. The random nanocomposites with enhanced local responses can be applied in different kinds of spectroscopy, including single molecules SERS.⁴²⁻⁴⁴ It is well known that the fractal phenomena are demonstrated or revealed by the model of cluster-cluster aggregation and diffusion-limited aggregation. Since the shape and size of the desired materials can be easily tuned by a well-defined template matrix, different templates spring up, such as porous anodic alumina, block copolymers, carbon nanotubes, hybrid organic-inorganic mesoporous materials, micelles and track-etch polycarbonate membranes.⁴⁵⁻⁴⁷ In 2015, Cinelet investigated the effect of fractal nano-antennas on the increase in SERS signal intensity through simulation to design substrates for SERS by E-beam lithography with highly predictable, repeatable, and sensitive substrates.⁴⁸ Figure 6 shows the fabricated Au-SiO₂-Au nano-cone arrays and its relevant simulation results of the electric field distribution at both Stokes wavelengths and the excitation is expressed in Figure 7. It elucidates that at the tip of the triangles and the gaps the intensified E-field of both wavelengths lead to definitely distinctive enhancement of SERS. The increment in the SERS signal intensity for fractal nano-antennas is own to in the cavities of the fractal structure hotspots are generated as a result of between the sub wave length features the plasmonic coupling.

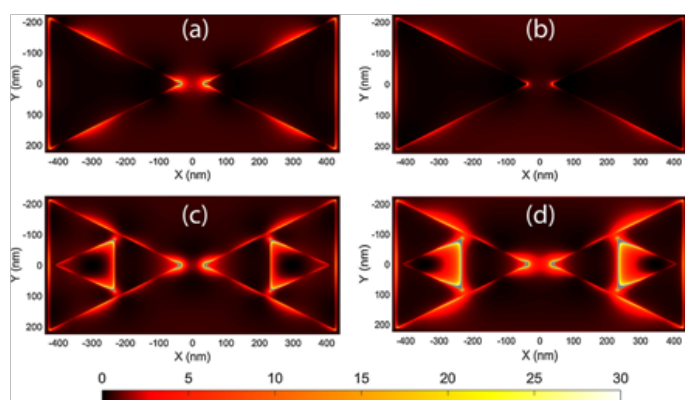


Figure 7 Electric field distributed at the laser (a, c) and Stokes shifted wavelength (b, d) 785 nm and 895 nm, respectively.

Xu et al.⁴⁹ calculated the fractal dimension of copper nano branches for SERS effect under 5 μ A direct current electric field using fast ionic conductor $\text{Rb}_4\text{Cu}_{16}\text{Cl}_{13}\text{I}_7$ films by a solid-state ionics method. The simulation results are shown in Figure 8. It indicates that the close degree of the dendritic copper nanostructures can be directly established by fractal calculation, rather than the conventional method by eye view which is extraordinary uncertainty. Moreover, the mechanism of copper nanostructures growth is revealed convincingly. As a result, the dendritic copper nanostructures can effectively enhance the SERS detection sensitivity and have extremely crucial importance for the trace analysis in chemistry, biology, medicine, and other fields. For SERS, Ag nanodendrites are always fabricated with natural and large fractal aggregates. The nascent small Ag nanoparticles may be active enough to undergo oriented attachment. At the same time, the concentration gradient of the Ag nanocrystal precursors sets up a uniform diffusion front, resulting in the preferential crystal orientations and symmetrical dendrites formation. Due to the dominant effect of diffusion and less active Ag nanocrystals, the angles of the branch/sub branch and stem/branch distinctively vary widely, and the differences of concentration in various growth sites are large. An asymmetrical dendrites are consequently fabricated. SERS results indicate when pyridine is taken as a probing molecule Raman scattering is enhanced and intensive for the Ag nanodendrites.⁵⁰

As a candidate for SERS-active substrates, Ag flowerlike nano fractals are also explored.^{51–55} Results shows that the flowerlike structures can strongly improve SERS enhancement due to the high density of the flowerlike with a lot of horns structures on Si substrate. It finds that near the interstitial areas of the leaves there are many hot spots through the local electromagnetic field distribution detection around the leaves of the flower. Even the interstitial areas are relative close between nanoparticles and leaves, a weak enhancement are still detected in the local electromagnetic filed. For a longer distance, weaker interaction exists and the interstitial nanoparticles areas have a very weak interaction. Therefore, the local electromagnetic field enhancement of the leaves interaction is stronger than that of nanoparticles. Furthermore, more complex Au with Ag flower like nanostructures have been fabricated by the eco-friendly method.⁵⁶ The flowerlike nanostructures are composed of blocks of 2D flake like nanostructures. Such Au flowerlike nano structures are stronger than those from other particle films and possess strong SERS effects attributed to their morphology.

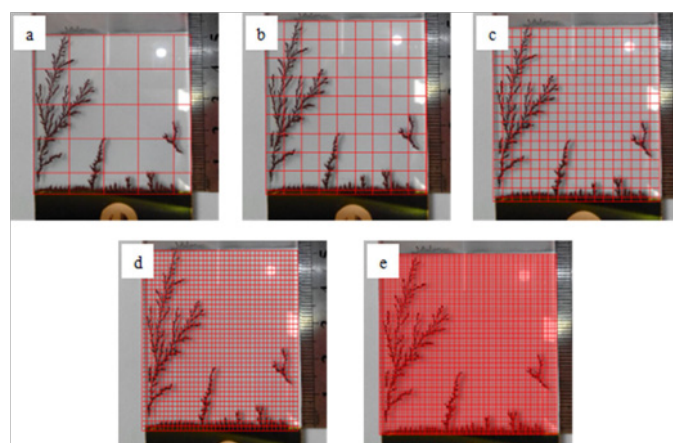


Figure 8 Cu nanostructures grids number (a) $r = 1$, $N = 17$; (b) $r = 0.5$, $N = 45$; (c) $r = 0.25$, $N = 115$; (d) $r = 0.125$, $N = 280$; (e) $r = 0.0625$, $N = 686$, respectively. Where, grids with various lengths ($r = 2^i$, $i = 0, 1, 2, \dots$ and $2^i < \text{the length of the image}$); the number of the grids: $N(r)$.

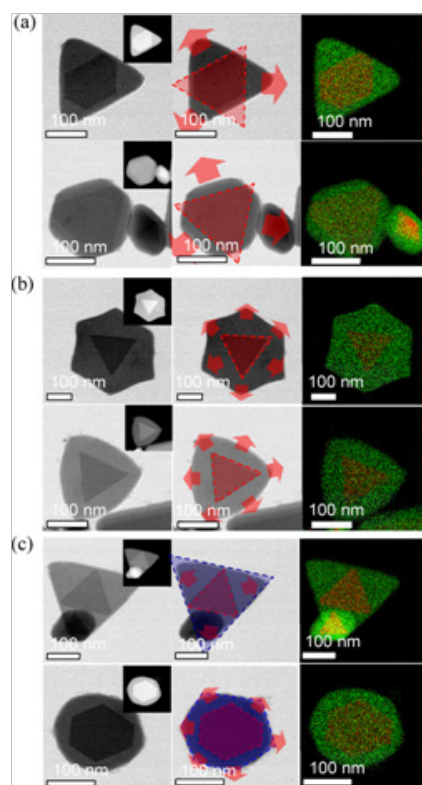


Figure 9 Silver-coated gold nanoparticles (hexagonal platelet, triangular prisms) STEM (bright- and dark-field) images and EDS maps (red: gold, green: silver): (a) silver shell formed from gold edges and growth from the missing corners is prohibited, (b) growth from the corners is allowed, and (c) an inverse structure is formed.

Nanoprisms

Because 2D assemblies of nano building blocks with ordered structures possess the optical, the magnetic and collective electronic properties distinctly different from those of the individual nanoparticles or the bulk solid, they are applied in a various important fields. But,

the assembly of isotropic spherical structures is the key issue which most research put efforts in. Up to now, because anisotropic assembly of anisotropic nanoobjects into controlled structures expresses new or improved properties relied on the assembly direction, spatial arrangement, and the order degree among the individual building blocks, it attracts more attention.^{57–60} Hayakawa and his coworkers investigated the tuned triangular silver-coated gold (Au@Ag) nanoprisms, plasmonic nanoparticles, with various sizes for SERS.⁶¹ The effect of the morphology of Au nanoprism on the growth of Ag out layer is shown in Figure 9. It reveals that the planes of edges must be different from the missing corners planes, and the growth from the missing corners is not supposed to be preferable, regardless of corner sharpness. As a result, the corner shape affects the last morphology. It demonstrates that when the Ag shell covers with the corners of the Au nanoprisms, the corners growth starts. But, because the edges growth speed is faster than that from the corners, hexagonal plates are dominant. If the Ag shell is pinned by the sharp corner tips, and an inverse triangle containing the Au nanoprism forms as shown in Figure 9c. Thus, this attractive structures with controlled arrangements possess obvious crystallographic, optical and SERS properties relied on their orientation in the assemblies, which is positively applicable to SERS substrates for environmental analysis and bio-logical uses. It should be noted that chemical approaches definitely lead to disordered systems resulted in uneasily manipulated or used for predictable and reproducible SERS enhancement although these methods can make nanoprisms with sharp corners,.

Hybrid nanostructures

Besides metal nanoprisms, in order to make strong SERS effects more complex nanostructures have already been explored.^{62–70} During SERS imaging, the magnetic field controls the nanocrescents suspended in the fluids. The Raman enhancement factor of a single nanocrescent is sufficient for high resolution biomolecular sensing in living cells due to that as high as those reported for nanoparticle clusters. Moreover, in dynamic SERS detection the signal-to-noise ratio of the nanocrescent orientation modulation adjusted by magnetic fields can be further increased. Although the anisotropic nanostructures fabrication for SERS have been taken substantial progress in the relevant technical innovation, a lot of gaps still exist in the roadmap of practical and successful SERS-based systems before these techniques are extensively explored. The crucial issue is that anisotropic assembly of anisotropic nanoobjects into the ordered structures is still a significant but hard to control task since they have new or enhanced properties relying on the spatial arrangement, the direction of assembly and the degree of order among the individual building blocks.

Conclusion

Surface enhanced Raman scattering (SERS) is attractively promising candidate for highly sensitive biological and chemical detection. Surfaces with functioned nanostructures tremendously enhance the surface plasma resonance for mation, such as nanorods and nanobranches/wires, nano fractal, nanoprisms, and hybrid nanostructures. Numerous substantial improvements in SERS fabrication with anisotropic nanostructures. However, effective controlling anisotropic nanoobjects assembly into ordered structures is a distinctive obstacle because the degree of order among the individual building blocks, spatial arrangement and the assembly direction determine the new and/or improved properties. Therefore, coupled

with the unique nanostructures approach the substantial enhancement in detectable Raman signal has made SERS extremely significant method for the trace analysis in chemistry, biology, medicine and other fields. Meanwhile, the optimization of the sensing system with the designed nanostructures should be deeply explored to agree with the requirements of environmental applications. To date, highly sensitive, durable and reproducible SERS substrates are still the major concerns in the practical applications, especially for the development of definitely efficient sensors to be used in complex environmental situations. Moreover, efforts should be put into exploring effective SERS sensor for much more toxic detection safely. Progress in the synthesis of multifunctional metal nanostructures with shape and size tailored, as well as the portable separation technique exploration is imminently supposed to explore to overcome the current limitations and advance the relevant technique applications further.

Acknowledgments

None.

Conflict of interest

The authors declare, that there is no conflict of interest.

Funding

None.

References

1. Fleischmann M, Hendra PJ, McQuillan AJ. Raman spectra of pyridine adsorbed at a silver electrode. *Chemical Physics Letters*. 1974; 26(2):163–166.
2. Keum JW, Kim MS, Park JM, et al. DNA-directed self-assembly of three-dimensional plasmonic nanostructures for detection by surface-enhanced Raman scattering (SERS). *Sensing and Bio-Sensing Research*. 2014;1:21–25.
3. Kundu S, Dai W, Chen YY, et al. Shape-selective catalysis and surface enhanced Raman scattering studies using Ag nanocubes, nanospheres and aggregated anisotropic nanostructures. *Journal of Colloid and Interface Science*. 2017;498:248–262.
4. Zhou QT, Thokchom AK, Kim DJ, et al. Inkjet-printed Ag micro-/nanostructure clusters on Cu substrates for in-situ pre-concentration and surface-enhanced Raman scattering. *Sensors and Actuators B*. 2017;243:176–183.
5. Dies H, Raveendran J, Escobedo C, et al. Experimental demonstration of the electromagnetic mechanism underlying surface enhanced Raman scattering using single nanoparticle spectroscopy. *Journal of Photochemistry and Photobiology A: Chemistry*. 2011;219 (2–3):167–179.
6. Guillot N, Lamy de la Chapelle M. The electromagnetic effect in surface enhanced Raman scattering: Enhancement optimization using precisely controlled nanostructures. *Journal of Quantitative Spectroscopy and Radiative Transfer*. 2012;113(18): 2321–2333.
7. Yamamoto YS, Ozaki Y, Itoh T. Recent progress and frontiers in the electromagnetic mechanism of surface-enhanced Raman scattering. *Journal of Photochemistry and Photobiology C: Photochemistry Reviews*. 2014;21:81–104.
8. Krajczewski J, Kołtąj K, Pietrasik S, et al. Silica-covered star-shaped Au–Ag nanoparticles as new electromagnetic nanoresonators for Raman characterisation of surfaces. *Spectrochimica Acta Part A: Molecular and Biomolecular Spectroscopy* 2018;193:1–7.

9. Hamon C, Liz-Marzán LM. Colloidal design of plasmonic sensors based on surface enhanced Raman scattering. *Journal of Colloid and Interface Science*. 2018;512:834–843.
10. Pandey GK, Pathak NK, Uma R, et al. Electromagnetic study of surface enhanced Raman scattering of plasmonic–biomolecule: An interaction between nanodimer and single biomolecule. *Solid State Communications*. 2017;255–256:47–53.
11. Dies H, Raveendran J, Escobedo C, et al. Rapid identification and quantification of illicit drugs on nanodendritic surface–enhanced Raman scattering substrates. *Sensors and Actuators B*. 2018;257:382–388.
12. Hermoso W, Alves TV, de Oliveira CCS, et al. Triangular metal nanoprisms of Ag, Au, and Cu: Modeling the influence of size, composition, and excitation wavelength on the optical properties. *Chemical Physics*. 2013;423:142–150.
13. Ankudze B, Philip A, Pakkanen TT, et al. Highly active surface–enhanced Raman scattering (SERS) substrates based on gold nanoparticles infiltrated into SiO₂ inverse opals. *Applied Surface Science*. 2016;387:595–602.
14. Mirsaleh-Kohan N, Duplanty M, Torres M, et al. Raman scattering of Cisplatin near silver nanoparticles. *Optics Communications*. 2018;410:228–231.
15. Chang TL, Yu XJ, Liang JF. Polydopamine–enabled surface coating with nano–metals. *Surface and Coatings Technology*. 2018; 337:389–395.
16. Zhang DJ, Fang JX, Li T. Sensitive and uniform detection using Surface–Enhanced Raman Scattering: Influence of colloidal–droplets evaporation based on Au–Ag alloy nanorods. *Journal of Colloid and Interface Science*. 2018;514:217–226.
17. Wang YT, Lee KC. The correlation between surface plasma resonance and surface enhanced Raman scattering. *Surface Science*. 1988;197:1–2:239–249.
18. Chang CC, Yang KH, Liu YC, et al. Surface–enhanced Raman scattering–active silver nanostructures with two domains. *Analytica Chimica Acta*. 2012;709:91–97.
19. Farcau C, Astilean S. Periodically nanostructured substrates for surface enhanced Raman spectroscopy. *Journal of Molecular Structure*. 2014;1073:102–111.
20. Chen HC, Hsu TC, Liu YC, et al. New sample preparation procedure for effective improvement on surface–enhanced Raman scattering effects. *Journal of Electroanalytical Chemistry*. 2014;724:48–54.
21. Laariedh F, Sow I, Ferchichi A, et al. Large–area, cost–effective Surface–Enhanced Raman Scattering (SERS) substrates fabrication. *Microelectronic Engineering*. 2015;145:124–127.
22. Nguyen AH, Lee JW, Choi HI, et al. Fabrication of plasmon length–based surface enhanced Raman scattering for multiplex detection on microfluidic device. *Biosensors and Bioelectronics*. 2015;70:358–365.
23. Sivashanmugan K, Liao JD, Liu BH, et al. Focused–ion–beam–fabricated Au nanorods coupled with Ag nanoparticles used as surface–enhanced Raman scattering–active substrate for analyzing trace melamine constituents in solution. *Analytica Chimica Acta*. 2013;800:56–64.
24. Jiji SG, Gopchandran KG. Au–Ag hollow nanostructures with tunable SERS properties. *Spectrochimica Acta Part A: Molecular and Biomolecular Spectroscopy*. 2017;171:499–506.
25. Suarasan S, Licarete E, Astilean S, et al. Probing cellular uptake and tracking of differently shaped gelatin–coated gold nanoparticles inside of ovarian cancer cells by two–photon excited photoluminescence analyzed by fluorescence lifetime imaging (FLIM). *Colloids and Surfaces B: Biointerfaces*. 2018;166:135–143.
26. Pal AK, Mohan DB. The Study of Surface Plasmon Enhanced Emission of ZnONanorods on Plasmonic Ag Nanorods Array. *Materials Today: Proceedings*. 2015;2(9):4407–4412.
27. Liaw JW, Lo WJ, Lin WC, et al. Theoretical study of optical torques for aligning Ag nanorods and nanowires. *Journal of Quantitative Spectroscopy and Radiative Transfer*. 2015;162:33–142.
28. Chang YC. Low temperature and large–scale growth of Zn Onanoneedle arrays with enhanced optical and surface–enhanced Raman scattering properties. *Sensors and Actuators B: Chemical*. 2016;225:498–503.
29. Park JH, Joo YL. A facile precursor route to highly loaded metal/ceramic nanofibers as a robust surface–enhanced Raman template. *Applied Surface Science*. 2017;416:742–750.
30. Belhaj M, Dridi C, Habba YG, et al. Surface morphology evolution with fabrication parameters of ZnO nanowires toward emission properties enhancement. *Physica B: Condensed Matter*. 2017;526:64–70.
31. Ta QTH, Park SH, Noh JS. Ag nano wire/ZnOnanobush hybrid structures for improved photocatalytic activity. *Journal of Colloid and Interface Science*. 2017;505:437–444.
32. Shang B, Wang YB, Yang P, et al. Synthesis of super hydrophobic polydopamine–Ag microbowl/nanoparticle array substrates for highly sensitive, durable and reproducible surface–enhanced Raman scattering detection. *Sensors and Actuators B*. 2018;255:995–1005.
33. Wu TH, Lin YW. Surface–enhanced Raman scattering active gold nanoparticle/nanohole arrays fabricated through electron beam lithography. *Applied Surface Science*. 2018;435:1143–1149.
34. Jani AMM, Losic D, Voelcker NH. Nanoporous anodic aluminium oxide: Advances in surface engineering and emerging applications. *Progress in Materials Science*. 2013;58(5):636–704.
35. Celik M, Altuntas S, Buyukserin F. Fabrication of nanocrater–decorated anodic aluminum oxidemembranes as substrates for reproducibly enhanced SERS signals. *Sensors and Actuators B*. 2018; 255:2871–2877.
36. Zhang CY, Lu Y, Zhao B, et al. Facile fabrication of Ag dendrite–integrated anodic aluminum oxidemembrane as effective three–dimensional SERS substrate. *Applied Surface Science*. 2016;377:167–173.
37. Kim YT, Schilling J, Schweizer SL, et al. High density Ag nanobranches decorated with sputtered Au nanoparticles for surface–enhanced Raman spectroscopy. *Applied Surface Science*. 2017;410:525–529.
38. Chursanova MV, Germash LP, Yukhymchuk VO, et al. Optimization of porous silicon preparation technology for SERS applications. *Applied Surface Science*. 2010;256(11):3369–3373.
39. Dridi H, Haji L, Moadhen A. Studies of SERS efficiency of gold coated porous silicon formed on rough silicon backside. *Applied Surface Science*. 2017;426:1190–1197.
40. Flores Romero E, Rodríguez Sevilla E, Cheang Wong JC. Silver films over silica microspheres (AgFOSM) as SERS substrates. *Photonics and Nanostructures–Fundamentals and Applications*. 2018;28:81–87.
41. Mandelbrot B. How long is the coast of Britain? Statistical self–similarity and fractional dimension. *Science*. 1967;156:636–638.
42. Cho FH, Lin YC, Lai YH. Electrochemically fabricated gold dendrites with high–index facets for use as surface–enhanced Raman–scattering–active substrates. *Applied Surface Science*. 2017;402:147–153.
43. Zhu XY, Wang AJ, Chen SS, et al. Facile synthesis of AgPt@Ag core–shell nanoparticles as highly active surface–enhanced Raman scattering substrates. *Sensors and Actuators B: Chemical*. 2018;260: 945–952.
44. Shapril NN, Ming CK, Said SM, et al. Optimization of silver

- nanodendrites for surface enhanced Raman spectroscopy (SERS) in an acidic environment. *Optik*. 2018;164:297–302.
45. Duy PK, Yen PTH, Chun S, et al. Carbon fiber cloth-supported Au nanodendrites as a rugged surface-enhanced Raman scattering substrate and electrochemical sensing platform. *Sensors and Actuators B: Chemical*. 2016;225:377–383.
 46. Hong JH, Kawashima A, Hamada N. A simple fabrication of plasmonic surface-enhanced Raman scattering (SERS) substrate for pesticide analysis via the immobilization of gold nanoparticles on UF membrane. *Applied Surface Science*. 2017;15:440–446.
 47. Yuan YF, Panwar N, Yap SHK, et al. SERS-based ultrasensitive sensing platform: An insight into design and practical applications. *Coordination Chemistry Reviews*. 2017;337:1–33.
 48. Cinel NA, Cakmakyapan S, Butun S, et al. E-Beam lithography designed substrates for surface enhanced Raman spectroscopy. *Photonics and Nanostructures-Fundamentals and Applications*. 2015;15:109–115.
 49. Xu DP, Dong J, Zhang S, et al. Fractal theory study and SERS effect of centimeter level of copper nano branch detectors by solid-state ionic method. *Sensors and Actuators A*. 2018;271:18–23.
 50. Cao Q, Yuan KP, Yu J, et al. Ultrafast self-assembly of silver nanostructures on carbon-coated copper grids for surface-enhanced Raman scattering detection of trace melamine. *Journal of Colloid and Interface Science*. 2017;490:23–28.
 51. Yang JH, Dennis RC, Sardar DK. Room-temperature synthesis of flowerlike Ag nanostructures consisting of single crystalline Ag nanoplates. *Materials Research Bulletin*. 2011;46(7):1080–1084.
 52. Upender G, Sathyavathi R, Raju B, et al. SERS study of molecules on Ag nanocluster films deposited on glass and silicon substrates by cluster deposition method. *Journal of Molecular Structure*. 2012;1012:56–61.
 53. Bian JC, Shu SW, Li JF, et al. Reproducible and recyclable SERS substrates: Flower-like Ag structures with concave surfaces formed by electrodeposition. *Applied Surface Science*. 2015;333:126–133.
 54. Qiu HW, Wang MQ, Jiang SZ, et al. Reliable molecular trace-detection based on flexible SERS substrate of graphene/Ag-nanoflowers/PMMA. *Sensors and Actuators B: Chemical*. 2017;249:439–450.
 55. Newmai MB, Verma M, Kumar PS. Monomer functionalized silica coated with Ag nanoparticles for enhanced SERS hotspots. *Applied Surface Science*. 2018;440:133–143.
 56. Wang RJ, Yao YF, Shen M, et al. Green synthesis of Au@Ag nanostructures through a seed-mediated method and their application in SERS. *Colloids and Surfaces A: Physicochemical and Engineering Aspects*. 2016;492:263–272.
 57. Herrera MA, Jara GP, Villarroel R, et al. Surface enhanced Raman scattering study of the antioxidant alkaloid boldine using prismatic silver nanoparticles. *Spectrochimica Acta Part A: Molecular and Biomolecular Spectroscopy*. 2014;133:591–596.
 58. Pilipavicius J, Kaleinikaite R, Pucetaite M, et al. Controllable formation of high density SERS-active silver nanoprism layers on hybrid silica-APTES coatings. *Applied Surface Science*. 2016;377:134–140.
 59. Bryche JF, Tsigara A, Béliier B, et al. Surface enhanced Raman scattering improvement of gold triangular nanoprisms by a gold reflective underlayer for chemical sensing. *Sensors and Actuators B: Chemical*. 2016;228:31–35.
 60. Chook SW, Yau SX, Chia CH, et al. Carboxylated-nanocellulose as a template for the synthesis of silver nanoprism. *Applied Surface Science*. 2017;422:32–38.
 61. Noda Y, Asaka T, Fudouzi H, et al. Accumulation and interparticle connections of triangular Ag-coated Au nanoprisms by oil-coating method for surface-enhanced Raman scattering applications. *Applied Surface Science*. 2018;435:687–698.
 62. Wang YJ, Jin AZ, Quan BG, et al. Large-scale Ag-nanoparticles/ Al_2O_3 /Au-nanograting hybrid nanostructure for surface-enhanced Raman scattering. *Microelectronic Engineering*. 2017;172:1–7.
 63. Kim NH, Kim S, Choi MS, et al. Combination of periodic hybrid nanopillar arrays and gold nanorods for improving detection performance of surface-enhanced Raman spectroscopy. *Sensors and Actuators B: Chemical*. 2018;258:18–24.
 64. Parmar V, Kanaujia PK, Bommali RK, et al. Efficient Surface Enhanced Raman Scattering substrates from femtosecond laser based fabrication. *Optical Materials*. 2017;72:86–90.
 65. Benítez Martínez S, López Lorente ÁI, Valcárcel M. Multilayer graphene-gold nanoparticle hybrid substrate for the SERS determination of metronidazole. *Microchemical Journal*. 2015;121:6–13.
 66. Sierra-Martin B, Fernandez-Barbero A. Inorganic/polymer hybrid nanoparticles for sensing applications. *Advances in Colloid and Interface Science*. 2016;233:25–37.
 67. Wang XY, Wang N, Gong TC, et al. Preparation of graphene-Ag nanoparticles hybrids and their SERS activities. *Applied Surface Science*. 2016;387:707–719.
 68. Wang XL, Wang M, Jiang T, et al. Dual-functional Fe_3O_4 @ SiO_2 @Ag triple core-shell microparticles as an effective SERS platform for adipokines detection. *Colloids and Surfaces A: Physicochemical and Engineering Aspects*. 2017;535:24–33.
 69. Bharadwaj S, Pandey A, Yagei B, et al. Graphene nano-mesh-Ag-ZnO hybrid paper for sensitive SERS sensing and self-cleaning of organic pollutants. *Chemical Engineering Journal*. 2018;336:445–455.
 70. Nair AK, Bhavitha KB, Perumbilavil S, et al. Multifunctional nitrogen sulfur co-doped reduced graphene oxide-Ag nano hybrids (sphere, cube and wire) for nonlinear optical and SERS applications. *Carbon*. 2018;132:380–393.